

# Digital hologram reconstruction using Rayleigh-Sommerfeld convolution method

Faye D. Espalmado\*

National Institute of Physics, University of the Philippines Diliman

\*Corresponding author: fdespalmado99@gmail.com

## Abstract

In this paper, we discuss the convolution method to record and reconstruct digital holograms. The effects of different parameters, namely the reconstruction wavelength, reconstruction distance, DC filter, central shifting filter, and hologram size, were explored in the reconstruction of a given sample experimental hologram. The hologram recording and reconstruction were also demonstrated using synthetically generated images. The parameters reconstruction distance and beam ratio were considered to be varied and observed. We extended the investigation on digital holography by reconstructing the hologram from Schnars and Juptner, (2002) using the Fresnel transform method.  
Keywords: digital holography, recording, reconstruction, convolution, Fresnel transform

## 1 Introduction

Holography relies on interference patterns to produce images wherein it offers the unique potential to capture the complete field information, i.e. amplitude and phase. This, in comparison to a photograph that only records the intensity, allows holograms to hold more depth and closely resemble an object.

Holography is generally a two-step process: 1) *recording* or writing the hologram, wherein the information amplitude and phase information is taken in by the recording medium and 2) *reconstructing* or reading the hologram, by which the hologram is illuminated with a reference field. In digital holography, the holograms are typically recorded by a charge-coupled device (CCD) and reconstructed by numerical methods such as the convolution method and Fresnel transform. The propagation of optical fields can be accurately described by diffraction theory, which allows numerical reconstruction of the image as an array of complex numbers representing the amplitude and phase of the optical field[1].

The convolution method to reconstruction utilizes the transfer function derived from the Rayleigh-Sommerfeld (RS) diffraction theory, where

$$U(x, y) = F^{-1}\{G_{RS}(x, y, d) \cdot F[U(x', y')]\} \quad (1)$$

and the RS transfer function given by:

$$G_{RS} = \exp\left[\left(i2\pi z/\lambda\right)\sqrt{1 - (\lambda f_x)^2 - (\lambda f_y)^2}\right] \quad (2)$$

where  $d$  corresponds to the distance,  $\lambda$  is the wavelength of the propagated optical field, and  $f_x$  and  $f_y$  are the spatial frequencies along the  $x$  and  $y$  axes, respectively[2]

## 2 Methodology

The digital holography simulations were conducted in MATLAB.

### 2.1 Reconstruction of an experimental hologram using the RS convolution method

The given the sample experimental hologram in Figure 1 will be reconstructed under various parameter configurations.

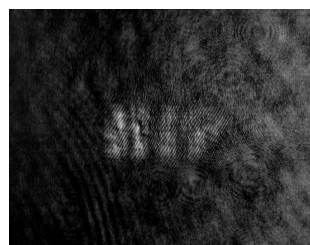


Figure 1: Experimental hologram

The scheme for the reconstruction of a hologram first starts with the removal of the zero-order diffraction or DC component by passing the hologram through a high-pass filter by fast Fourier transform. Then, the resulting spectrum is center-shifted to remove the carrier frequency and twin image. The RS convolution is then applied.

To demonstrate the numerical focusing in the amplitude and phase, we vary the observation distance  $z$  in the set-up. Other parameters varied to observe its effects on the phase and amplitude of the reconstructed wave are the reconstruction wavelength, DC filter window size, central shifting filter window size, and hologram size. In varying the DC filter, the central shifting process was skipped.

## 2.2 Holographic process: hologram recording and reconstruction

For the hologram recording, the input field red and undergoes the RS convolution. A tilted plane wave is introduced as a the reference beam. The sum of the intensity of the two fields corresponds to the interference of the two fields.

Different images were obtained to be recorded into a hologram. The circular aperture and a random distribution input field were generated. The image of crystallized amino acids was acquired from The Atlantic webpage[3].

Numerical focusing was also demonstrated with the varying reconstruction distances. We also investigated the effect of varying the beam ratio during the recording process on the quality of the hologram and reconstructed wave. The varied parameters were tested on a circular aperture input field.

## 2.3 Reconstruction of an experimental hologram using the Fresnel transform method

As an extension, we also reconstructed the digital hologram given in the paper, "Digital recording and numerical reconstruction of holograms" by Schnars and Juptner[4]. In this part, the reconstruction was conducted using Fresnel transform, instead of the convolution method used in the first parts of the experiment. The process were simulated with different reconstruction wavelength and observation distance to demonstrate the characteristic of automatic scaling in the Fresnel transform method.

## 3 Simulations and results

### 3.1 Reconstruction of an experimental hologram using the RS convolution method

#### 3.1.1 Varying observation distances

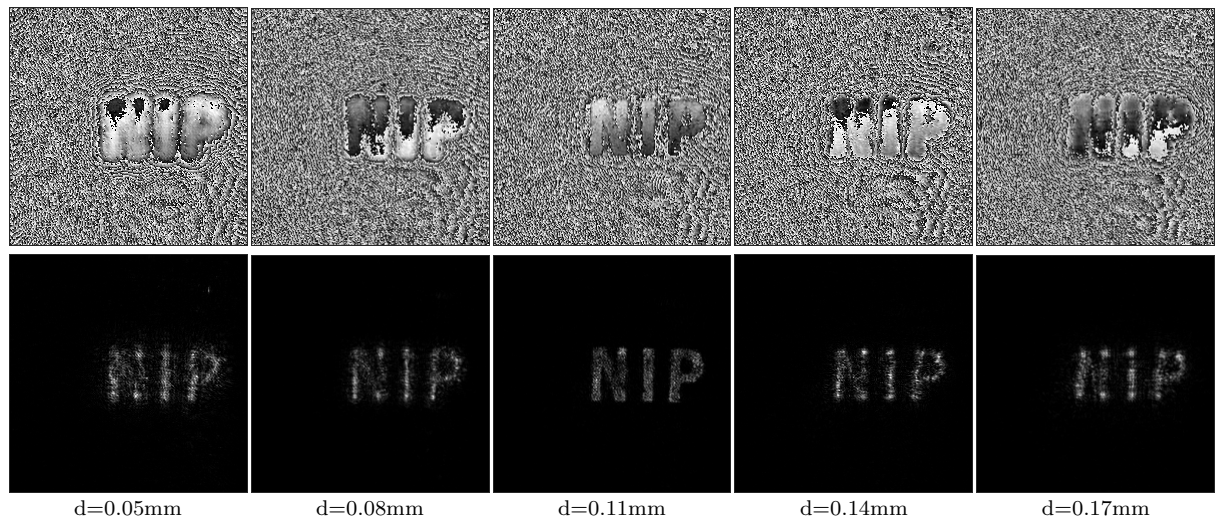


Figure 2: Phase distribution (top row) and the corresponding amplitudes (bottom row) for holographic reconstruction in different observation distances.

Figure 2 shows the numerical focusing as the observation distance increases. As shown in the amplitudes in the reconstructed wave, the image is blurred and more scattered at  $z=0.05\text{mm}$  then becomes more distinguished at  $z=0.11\text{mm}$  then proceeds to get blur again at the next distance values.

### 3.1.2 Varying reconstruction wavelengths

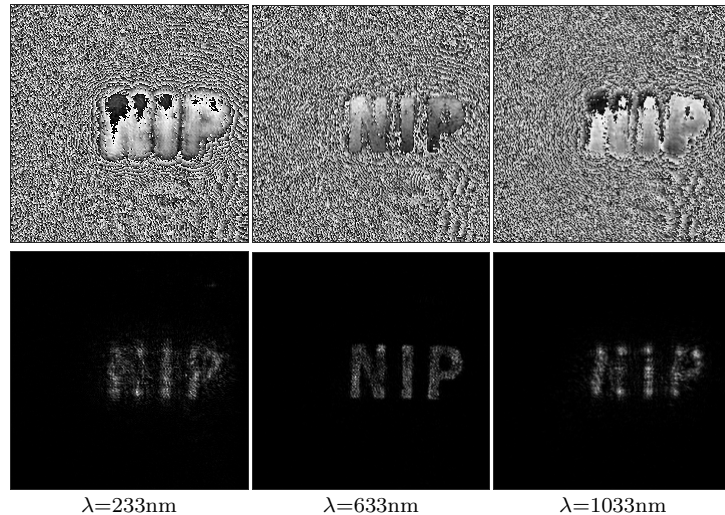


Figure 3: Phase distribution (top row) and the corresponding amplitudes (bottom row) for holographic reconstruction in different reconstruction wavelengths.

The pattern shown in Figure 3 for varying reconstruction wavelengths is similar to that in Figure 2 with the numerical focusing. The image in the amplitude is cleared in the 633nm wavelength while at 233nm and 1033nm the images is blurry and scattered.

### 3.1.3 Varying DC filter window sizes

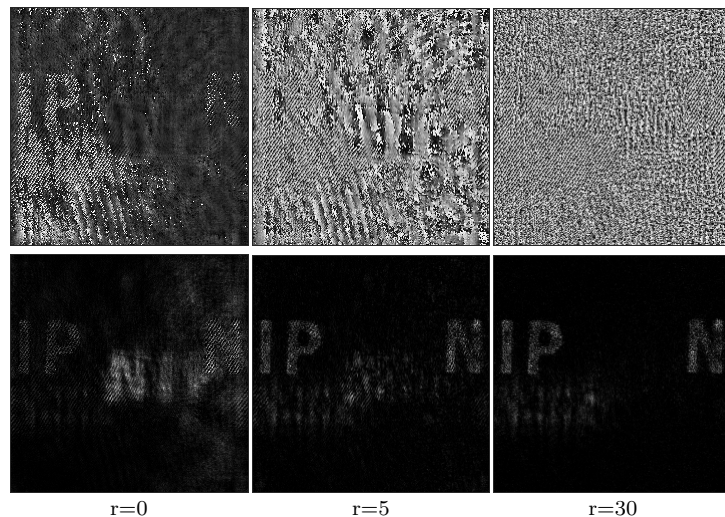


Figure 4: Phase distribution (top row) and the corresponding amplitudes (bottom row) for holographic reconstruction with different DC filter window sizes.

The central shifting filter was disabled during this part of the experiment, so the twin images and the carrier frequency was not removed. Hence, we can see the another set of letters at the side of the images in Figure 4. In the variation of the DC filter radius, we see that that as the radius increases, the letters in the middle of the amplitude images eventually fade. This can corresponds to the removal of the DC component in the image.

### 3.1.4 Varying CS filter window sizes

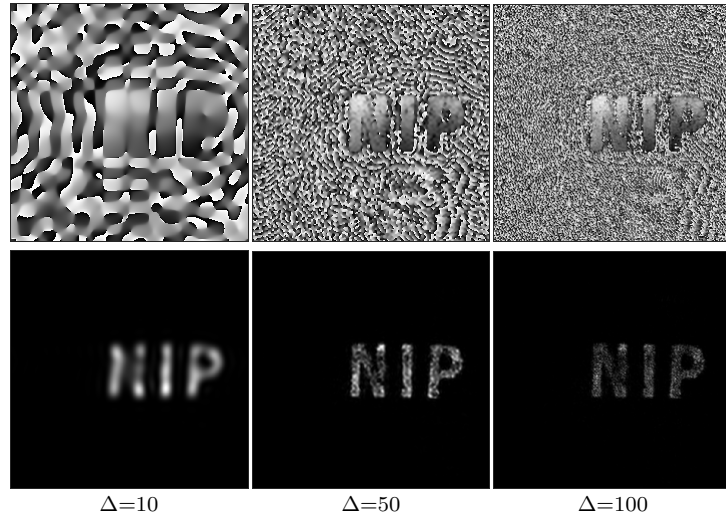


Figure 5: Phase distribution (top row) and the corresponding amplitudes (bottom row) for holographic reconstruction with different CS shifting filter window sizes.

In Figure 5, the size of window to be shifted to the center is tested. The phase distribution of the reconstructed waves illustrates an increasing number of fringes as the window size increases. In the output amplitudes, the letters become more clear as the window size increases, however, the brightness of the image decreases.

### 3.1.5 Varying hologram sizes

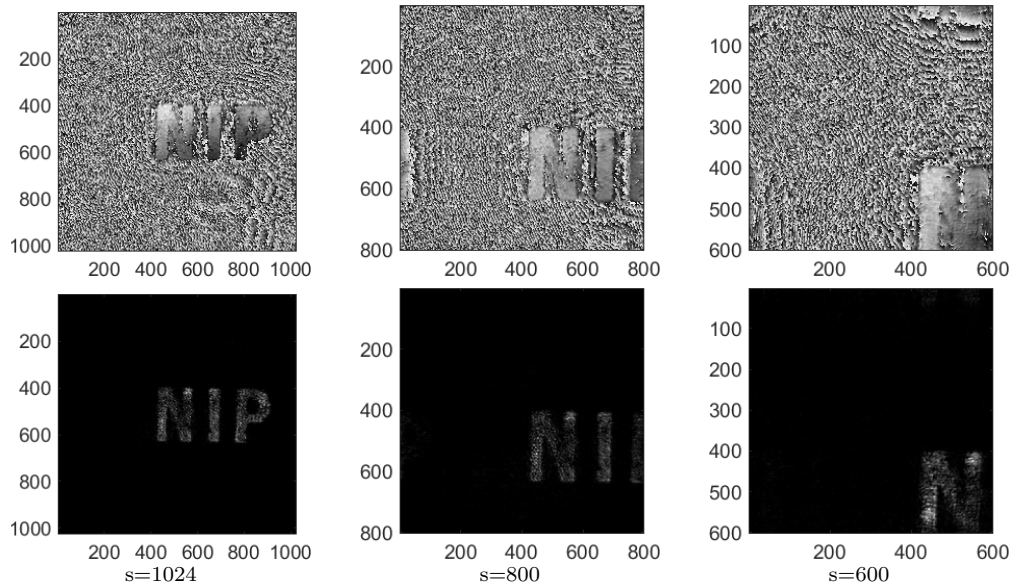


Figure 6: Phase distribution (top row) and the corresponding amplitudes (bottom row) for holographic reconstruction for different hologram sizes.

By changing the hologram size, we end up with choosing only portions of the whole image, and only the information from that portion is considered in the process of reconstruction. This is demonstrated in Figure 6, wherein we get finer details with a larger hologram size as compared to the smaller hologram sizes.

### 3.2 Holographic process: hologram recording and reconstruction

#### 3.2.1 Varying input fields for recording

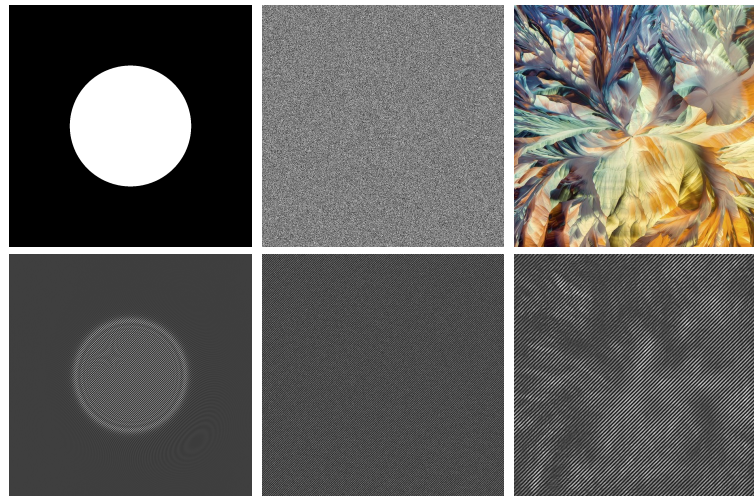


Figure 7: Different types of input fields (top row) and their corresponding holographic recordings (bottom row).

We have recorded the holograms for the different input fields shown in Figure 7. In all these holograms, there are visible parallel fringes along the diagonal of the images, seemingly following the pattern in the phase of the reference beam. Additionally, circular fringes can also be seen outside that of the central circle for the circular aperture.

#### 3.2.2 Varying reconstruction distances

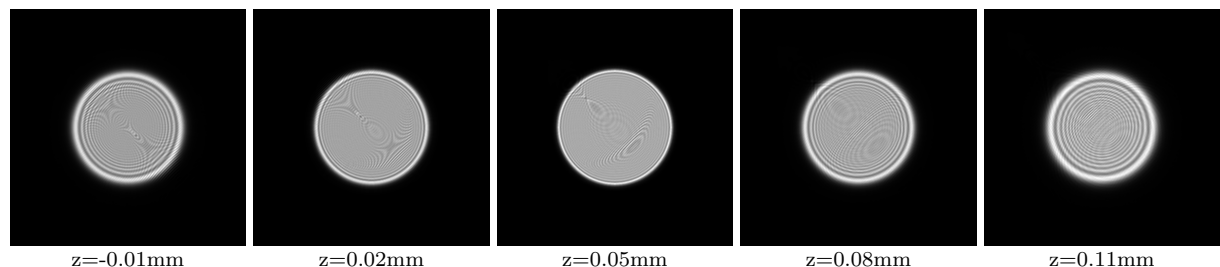


Figure 8: Holograph reconstruction of a circular aperture at different distances.

We can also observe the numerical focusing with the varying reconstruction distances in Figure 8. Specifically, we see higher contrast between the circular fringes in the leftmost and rightmost images in Figure 8. The fringe sizes are also wider and lesser in number in both the aforementioned images. The image at the center has higher number and lower contrast fringes among the simulated images at certain distances.

### 3.2.3 Varying beam ratio in the recording process

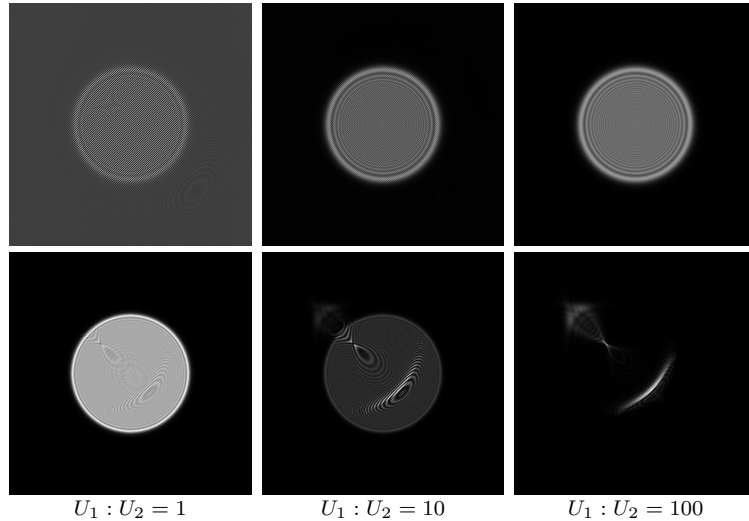


Figure 9: Hologram recording (top row) and corresponding reconstruction (bottom row) for different beam ratios.

From Figure 9, it is observed that all the reconstructed image have an almost similar fringe patterns. However, there is also a decreasing contrast with increasing beam ratio such that some of the fringe patterns are not visible anymore at the 100 ratio.

### 3.3 Reconstruction of an experimental hologram using the Fresnel transform method

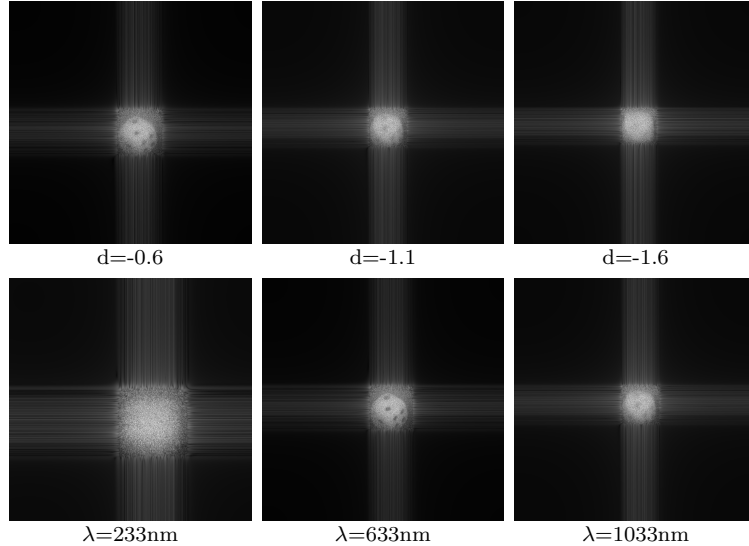


Figure 10: Dice hologram reconstruction with varying parameters: observation distance (bottom row), reconstruction wavelength (top row)

The simulated images in Figure 9 still also follows a numerical focusing scheme across the different tested parameters, wherein the dice is more visible or defined at the middle values of the parameter and gets blurred at the edge values. However, we can also observe a change in the scale of the images, which does not happen in the simulations using convolutional method. This is related to the the automatic scaling characteristic for the Fresnel transform method, described by the expression  $\Delta\xi = \lambda d / N \Delta x$ , where  $N$  is the number of pixels[4].

## 4 Conclusions

We have obtained the phase and amplitude of the reconstructed wave from a given experimental hologram. Furthermore, we have demonstrated the numerical focusing and effects of certain parameters. The process of recording and reconstructing a hologram was also conducted with different input fields. Different reconstruction distances and beam ratios was evaluated using a circular aperture input field.

Additionally, the Fresnel transform approach to numerical reconstruction of a dice hologram was performed. The automatic scaling in the method is also observed.

Further studies can still be conducted on the methods and applications of digital holography.

## References

- [1] M. K. Kim, Principles and techniques of digital holographic microscopy, *SPIE Reviews* **1**, 018005 (2010).
- [2] J. L. C. J. R. Sheppard and S. S. Kou, Rayleigh–sommerfeld diffraction formula in k space, *J. Opt. Soc. Am. A* **30**, 1180 (2013).
- [3] J. Zoll, Crystallized amino acids l-glutamine and beta-alanine, <https://www.theatlantic.com/photo/2019/10/photographing-microscopic-winners-nikon-small-world-2019/600403/>.
- [4] U. Schnars and W. P. Juptner, Digital recording and numerical reconstruction of holograms, *Meas. Sci. Technol.* **13**, R85–R101 (2002).